DESIGN, REALIZATION AND CHARACTERIZATION OF ALL-AROUND SiO_2/Al_2O_3 GATE, SUSPENDED SILICON NANOWIRE CHEMICAL FIELD EFFECT TRANSISTORS

Ahmet LALE[1], Auriane GRAPPIN[1], David BOURRIER[1], Laurent MAZENQ[1], Aurélie LECESTRE[1], Jérôme LAUNAY[1] and Pierre TEMPLE-BOYER[1]
[1]LAAS-CNRS, Université de Toulouse, F-31400 Toulouse, France

ABSTRACT

We present a sensor platform associated to silicon-nanowire chemical field effect transistors (Si-nw-ChemFET). Innovations concern the use of networks of suspended silicon $N^+/P/N^+$ nanowires as conducting channel, the realization by thermal oxidation and Atomic-Layer Deposition (ALD) of a SiO_2/Al_2O_3 gate insulator all-around the silicon nanowires, and their final integration into covered SU8-based microfluidic channels. The Si-nw-MOSFET/ChemFET fabrication process and electrical/electrochemical characterizations are presented. The fabrication process did not need an expensive and time-consuming e-beam lithography, but only fast and "low cost" standard photolithography protocols. Such microdevice will provide new opportunities for bio-chemical analysis at the micro/nanoscale.

KEYWORDS

ChemFET, finFET, MOSFET, ISFET, silicon nanowire, biosensor, potentiometric sensor, nanosensor, microsensor, pH measurement, microfluidics, gate all-around.

INTRODUCTION

Chemically sensitive Field Effect Transistors (ChemFET) are microsensors derived by Metal Oxide Semiconductor Field Effect Transistors [1]. These are electronic microsensors designed to measure the pH. ChemFETs have shown interesting properties for the detection in liquid phase [1][2] and have been functionalized for many applications such as the measurement of potassium [3], sodium [3], ammonium [4], urea [5], creatinine [6], lactate [7], glutamate [8]…

Nevertheless, to open the door to new innovative applications for ChemFET-based microsensors, it is necessary to increase their sensitivity, to decrease response times and their detection limit. To meet this challenge, the development of nanotransistor based on silicon nanowire Si-nw-ChemFET was proposed [9][10]. In this field, surrounding gate seems the ideal candidate: indeed, low channel dimensions provide new detection mechanisms as well as analysis of micro/nano-volumes, allowing to work at the single cell level [10]. Nevertheless, the development of suspended silicon nanowires should still improve Si-nw-ChemFET detection properties in liquid phase, providing the integration of well-controlled chemically-sensitive gate insulators all-around the Si-nw-based conductive channel.

EXPERIMENTAL

Device fabrication

6-inch SOI wafers (Silicon On Insulator, P type, 10^{15} atoms/cm^3) were used.

These devices consist in single and networked silicon nanowires field effect transistors. Different wire lengths, gate lengths and number of parallel wires were fabricated.

First, source and drain areas were N doped (10^{20} atoms/cm^3) with arsenic ion implantation. Two different gate length were realized, 0.9µm and 3,9µm.

To fabricate silicon nanowires, projection photolithography with a Canon FPA-3000i4 stepper and an AZ ECI 3012 photoresist were employed. After optimizations, were achieved on a single chip, with the same insolation parameters, patterns of transistors with a single nanowire as channel, next to patterns of transistors with 100 nanowires parallel network (figure 1). The goal is to compare in the future, the pros and cons of each structure, in terms of limit of detection and/or sensitivity for biochemical applications.

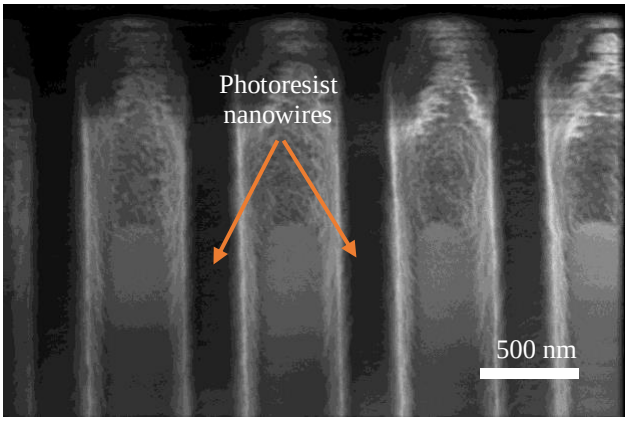

Figure 1: SEM view of a network of photoresist nanowires, before reactive ion etching (tilt 52°).

Once photoresist nanowires were optimized, nanopatterns were transferred in silicon thanks to a reactive ion etching. After optimization, 200nm x 170nm rectangle section nanowires were obtained with a perfect reproducibility. Two different densities of network were realized: 20 and 100 nanowires over a width of 80µm. Thus, using SOI wafers, networks of suspended silicon nanowires were successfully integrated.

Then the realization of the gate structure was performed. After RCA cleaning, a dry thermal oxidation of 22nm was achieved and an alumina film of 26nm was deposited by ALD. The advantage of this technique is to deposit extremely conformal films all around the nanowires, while providing well-controlled thicknesses [11]. Thus, a SiO_2/Al_2O_3 gate was integrated all-around the

silicon nanowire (figure 2). This Al_2O_3 layer was used as a gate chemically-sensitive layer as well as the microdevice passivation layer in liquid phase [9][12].

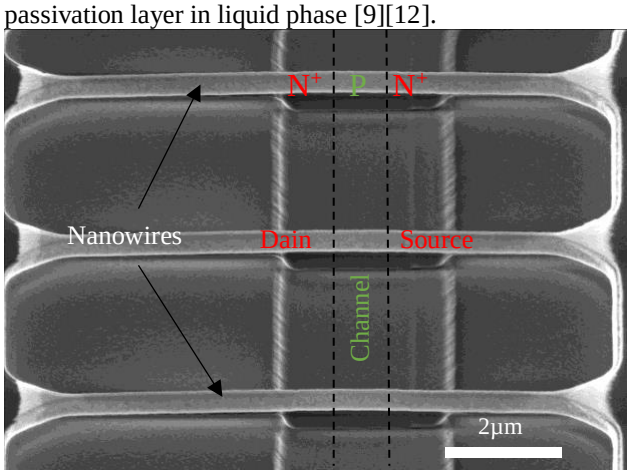

Figure 2: SEM view of silicon nanowires after gate insulator completion (tilt 52°).

Once the gate/source/drain metallic contacts and interconnections were ended, Si-nw-MOSFET and Si-nw-ChemFET were fabricated (figure 3).

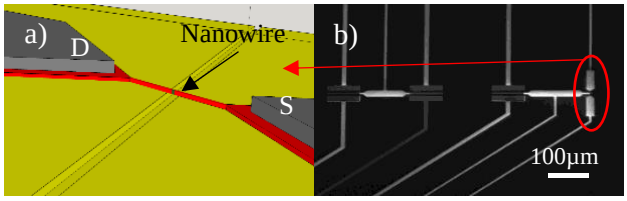

Figure 3: a) Schematic view and b) SEM view of the Si-nw-ChemFET with interconnections.

Then, using a specific SU8-3D technique [13], covered 5µm width microfluidic channels were finally realized in order to deal with liquid phase analysis at the microscale (figure 4).

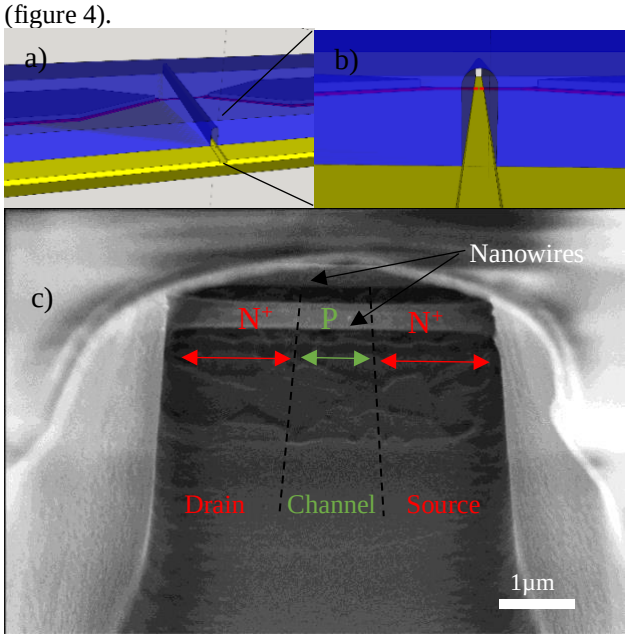

Figure 4: a) and b) schematic views of the Si-nw-ChemFET and the microfluidic channel. c) SEM view of suspended silicon nanowires inside a covered microfluidic channel (tilt 52°).

DEVICE CHARACTERIZATIONS

Si-nw-MOSFET/ChemFET were characterized electrically and electrochemically using standard I-V experiments (figure 5). The MOSFET works without liquid, so it makes easier some characterizations. It allows to check the quality of the manufacturing process, and to discriminate problems due to the transistor from those related to the microfluidics.

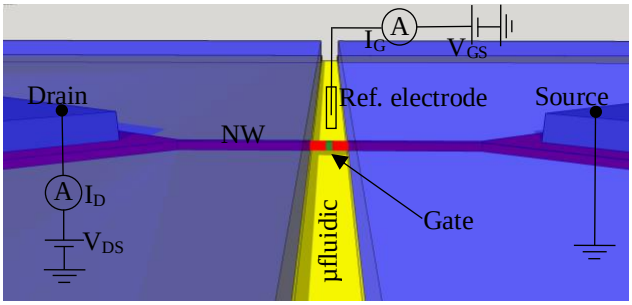

Figure 5: schematic view of the polarization for Si-nw-ChemFET characterizations.

Si-nw-MOSFET characterizations

The threshold voltage of 42 transistors was measured and the mean value was 0.62V with a standard deviation of only 0.26V (figure 6). That shows the quality of the SiO_2/ALD-Al_2O_3 gate dielectric and the Si/SiO_2 interface.

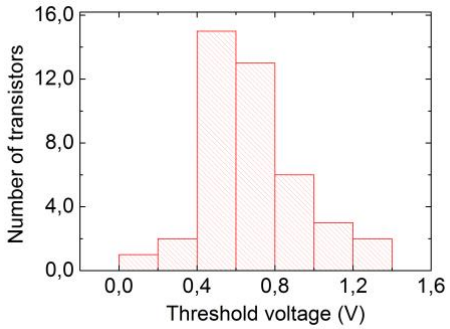

Figure 6 : distribution of the threshold voltage of the Si-nw-MOSFET.

The influence of 2 parameters on electric characteristics was studied: the number of parallel nanowires (1, 20 and 100) and the gate length L_G (0.9µm "short" and 3.9µm "long"), the length of the nanowires is 10µm.

Firstly, very low subthreshold (I_{OFF}) currents (7.10^{-14}A for V_{GS} = -2V, V_{DS} = 0.1V) were obtained for a parallel network of 100 nanowires (figure 7). This leakage current is the same for both gate lengths and proportional to the number of parallel nanowires. Therefore, it allows to estimate the leakage current of X nanowires.

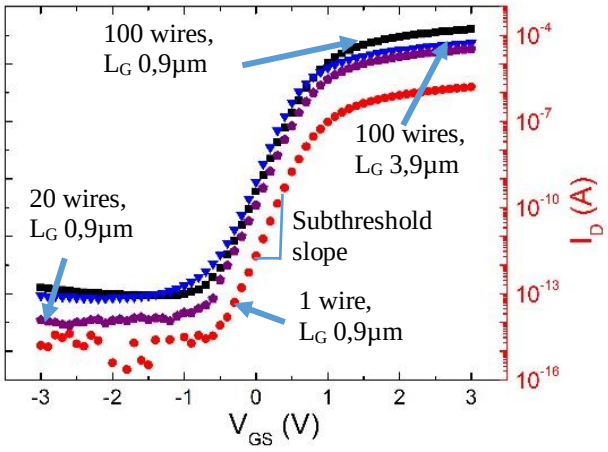

Figure 7: Id(Vgs) characterizations of Si-nw-MOSFETs, semi-logarithmic scale. (Vds = 0.1V)

The leakage current through the gate dielectric (I_G) is lower than 10^{-15}A (limits of the measuring instrument) for 100 parallel nanowires under 3V. So, the I_G current is lower than 10^{-17}A for one nanowire and shows the insulation quality of the SiO_2/Al_2O_3 double layer.

The number of parallel nanowires and the gate length does not influence the subthreshold slope, which is 6 decades/V.

The ratio I_{ON}/I_{OFF} is about 9 decades, thanks to the very low I_{OFF} current.

The transconductance is 4.3 times higher for nanowires with the short gate length in comparison with the long gate length, exactly the length ratio between the long and short gate lengths. The transconductance is also proportional to the number of parallel nanowires (figure 8).

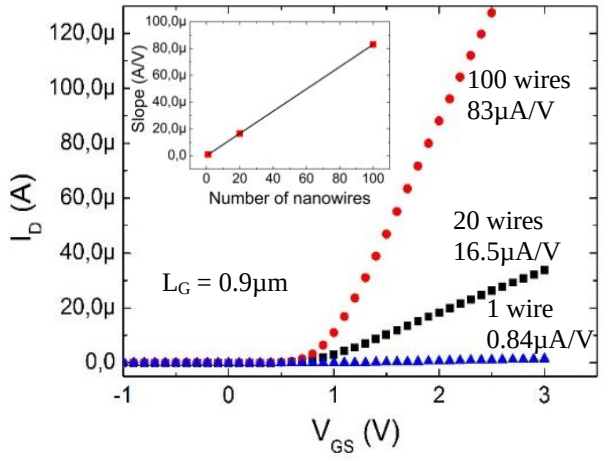

Figure 8: Id(Vgs) characterizations of Si-nw-MOSFETs, linear scale. (Vds = 0.1V)

All these characterizations have confirmed the well operation of Si-nw-MOSFET. The main characteristics are grouped in the table 1.

Table 1: evolution of the main characteristics with the gate length and the number of parallel nanowires for the Si-nw-MOSFET.

Structure	G_M or ON current	I_{ON}/I_{OFF}	Subthreshold slope
1 wire / L_G 3,9 µm	X	9.10^8	6 (decades/V)
1 wire / L_G 0,9µm	4,3.X	4.10^9	6 (decades/V)
100 wires / L_G 3,9µm	100.X	9.10^8	6 (decades/V)
100 wires / L_G 0,9µm	100.4,3.X	4.10^9	6 (decades/V)
20 wires / L_G 0,9µm	20.4,3.X	4.10^9	6 (decades/V)

Si-nw-ChemFET characterizations

The Si-nw-ChemFET is like a Si-nw-MOSFET which gate metallization is replaced by a microfluidic channel. Si-nw-ChemFETs were characterized in liquid phase with a specific setup. The liquid was polarized with an Ag/AgCl/KClsat double junction glass reference electrode.

Like for the study of Si-nw-MOSFET, the influence of 2 parameters on electric characteristics was studied: the number of parallel nanowires (1 and 100) and the gate length L_G (0.9µm "short" and 3.9µm "long"), the length of the nanowires is 10µm.

The subthreshold leakage current (I_{OFF}) and the leakage current through the gate dielectric (I_G), for 100 parallel nanowires, were not measurable because they were lower than the limit of the measuring instrument used (5.10^{-11}A) (figure 9). That means an I_{OFF} current and an I_G current lower than 5.10^{-13}A for one nanowire. These very low leakage currents allow a high I_{ON}/I_{OFF} ratio reaching at least 10^7 for one nanowire and 10^8 for 100 parallel nanowires.

Concerning the subthreshold slope, excellent characteristics were obtained, with 8 decades/V. Like for the Si-nw-MOSFET, this value is independent of the number of parallel nanowires and gate length. As for the Si-nw-ChemFET, the transconductance is inversely proportional to the gate length.

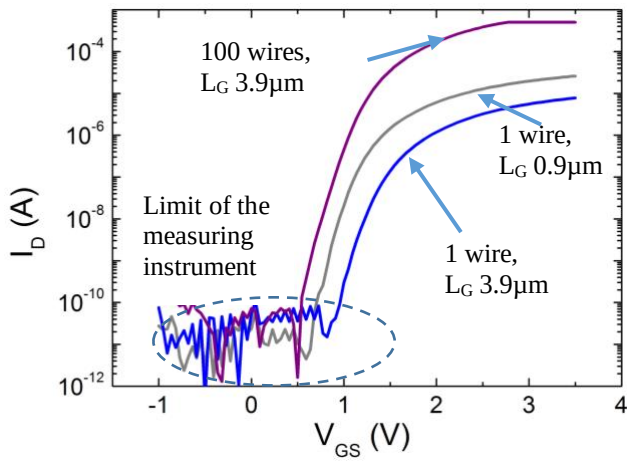

Figure 9 : Id(Vgs) characterizations in liquid phase of Si-nw-ChemFETs, with a semi-logarithmic scale.(Vds = 1V)

The Nernstian response to pH variations of 58mV/pH is in agreement with theory (figure 10). There is no sensitivity differences when the gate length or the number of parallel nanowires changes, no hysteresis in the pH responses and no sensitivity to interfering ions Na^+ and K^+ (results not shown).

All these characterizations have shown the well behavior of Si-nw-ChemFET in liquid phase, and demonstrated the performances of the bilayer SiO_2/ALD-Al_2O_3 for ChemFET fabrication.

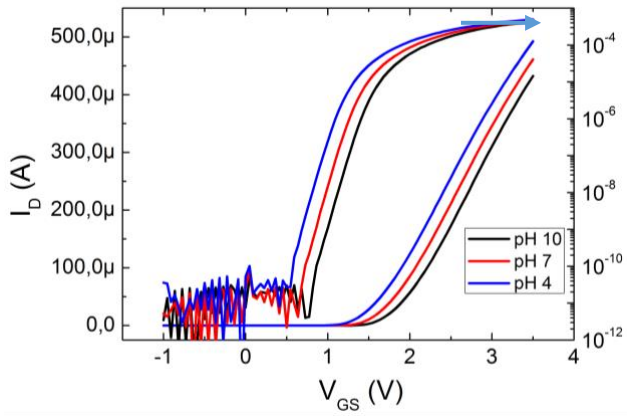

Figure 10: Id(Vgs) characterizations in liquid phase of Si-nw-ChemFET, with a semi-logarithmic and a linear scale, for three different pH.(Vds = 1V)

DISCUSSION

These good results are due to the excellent control of the nw-Si/insulator/electrolyte interface using an all-around gate with high dielectric capacity.

Junctions on the nanowires make possible to increase the I_{ON}/I_{OFF} ratio by decreasing strongly the current when the transistors are in their blocked mode.

The reduction of the gate length make possible to increase the transconductance, it is interesting for the amplification of biochemical signals like action potentials [14].

The bilayer SiO_2/Al_2O_3 is advantageous because the Si/SiO_2 allows a very good interface, which is highly important for a MOSFET based component. The second layer, the ALD-Al_2O_3 is a good (high-k) insulator in liquid phase. That is why gate leakage currents are so low. Thanks to Al_2O_3, Si-nw-ChemFET shows near Nernstian responses to pH changes without hysteresis and with selectivity against K^+ and Na^+ ions, which means more accuracy and sensitivity.

This allows to hope for a much better signal-to-noise ratio for biological applications than planar ChemFET.

CONCLUSION

Silicon nanowire based MOSFET and ChemFET (Si-nw-MOSFET and Si-nw-ChemFET) were designed, realized and presented in this paper. Electrical and electrochemical characterizations have shown good results.

In short-term perspective, thanks to the small dimensions of sensing area and to improved detection performances, the accurate and reproducible monitoring of biological metabolisms is expected on living cells using suspended Si-nw-ChemFET.

ACKNOWLEDGEMENTS

This work was partly supported by LAAS-CNRS micro and nanotechnologies platform, member of the French RENATECH network.

REFERENCES

[1] Bergveld, P. IEEE Transactions on Biomedical Engineering BME-17, 70–71 (1970).
[2] Fromherz, P. Solid-State Electronics 52 1364-1373 (2008).
[3] Hajji, B. et al. Microelectronics Reliability 40, 783–786 (2000).
[4] Humenyuk, I. et al. Microelectronics Journal 37, 475–479 (2006).
[5] Temple-Boyer, P. et al. Sensors and Actuators B: Chemical 131, 525–532 (2008).
[6] Sant, W. et al. Sensors and Actuators B: Chemical 103, 260–264 (2004).
[7] Diallo, A. K. et al. Biosensors and Bioelectronics 40, 291–296 (2013).
[8] Djeghlaf, L. (Université Paul Sabatier - Toulouse III, 2013).
[9] Knopfmacher, O. et al. Procedia Chem., vol. 1, no. 1 678–681, Sep. 2009.
[10] Duan X. et al. Nature Nanotechnology 7 174-179 (2012).
[11] Elam, J et al. Chemistry of materials 18 3507-3517 (2003).
[12] Matsuo, T. & Esashi, M. Sensors and Actuators 1, 77–96 (1981).
[13] Larramendy, F. et al. Sensors and Actuators B: Chemical 203, 375–381 (2014).
[14] Fromherz P, Chemphyschem 2002, 3, 276-284 (2002)

CONTACT

Pierre Temple-Boyer: temple@laas.fr